TECHNICAL REPORTS

nature medicine

# Orderly recruitment of motor units under optical control *in vivo*

Michael E Llewellyn[1], Kimberly R Thompson[1], Karl Deisseroth[1,2] & Scott L Delp[1,3]

**A drawback of electrical stimulation for muscle control is that large, fatigable motor units are preferentially recruited before smaller motor units by the lowest-intensity electrical cuff stimulation. This phenomenon limits therapeutic applications because it is precisely the opposite of the normal physiological (orderly) recruitment pattern; therefore, a mechanism to achieve orderly recruitment has been a long-sought goal in physiology, medicine and engineering. Here we demonstrate a technology for reliable orderly recruitment *in vivo*. We find that under optical control with microbial opsins, recruitment of motor units proceeds in the physiological recruitment sequence, as indicated by multiple independent measures of motor unit recruitment including conduction latency, contraction and relaxation times, stimulation threshold and fatigue. As a result, we observed enhanced performance and reduced fatigue *in vivo*. These findings point to an unanticipated new modality of neural control with broad implications for nervous system and neuromuscular physiology, disease research and therapeutic innovation.**



A typical muscle is comprised of many thousands of fibers that contain its contractile machinery. Rather than controlling each fiber individually, the nervous system controls motor units, which are groups of fibers innervated by a single motor neuron. These motor units vary in size, from several fibers to several thousand fibers, and in the type of constituent muscle fibers. Small motor units have small-diameter axons typically innervating slow muscle fibers that are fatigue resistant, whereas large motor units have large-diameter axons that typically innervate faster muscle fibers that are more fatigable[1,2]. In 1957, Elwood Henneman *et al.*[2,3] discovered that motor units are recruited in order, from small to large, with increasing levels of motor activation. Henneman's size principle has become one the major tenets of neurophysiology and provides the biophysical basis for the recruitment of the smallest, most fatigue-resistant fibers for tasks that require fine motor control over long periods of time while reserving larger motor units for brief bursts of high force production[4,5].

Small motor neurons have small cell bodies with fewer parallel ion channels and tend to have higher input resistance than large motor neurons[6]. Small motor neurons therefore respond to a given synaptic current with a greater change in membrane potential, causing them to reach the threshold for initiation of an action potential with less synaptic current than large motor neurons[6]. Under electrical stimulation of a motor nerve by a cuff, however, larger myelinated axons are typically recruited at lower applied voltages than smaller myelinated axons, although sometimes this order is more random (**Supplementary Methods**)[7–9]. This reverse or random recruitment order of motor units by electrical stimulation makes it difficult to modulate and maintain muscle force[10].

Recent discoveries have made it possible to stimulate mammalian neurons with pulses of light[11,12]. This is done by genetically inserting a photo-activatable protein into the desired neuron. For example, the membrane-targeted photoactivated cation channel channelrhodopsin-2 (ChR2) from the alga *Chlamydomonas reinhardtii* has enabled millisecond-precision control of central nervous system neurons in response to brief pulses of light[11,12]. We explored the possibility of recruiting motor neurons by photoactivation, reasoning that if photoactive channel density were similar in large and small axons, the higher input resistance of smaller motor neurons[6] would result in greater membrane potential changes in response to fixed conductance changes. Smaller motor units would then be activated before larger motor units, achieving the goal of orderly recruitment.

## RESULTS

### Characterization of *Thy1*::*ChR2* expression in mouse motor neurons

To achieve microbial opsin expression in peripheral nerves, we used a transgenic mouse line expressing the ChR2-YFP fusion protein under the *Thy1* promoter, which drives robust expression in neurons of both the central and peripheral nervous systems[13], including lower motor and dorsal root ganglion neurons (**Fig. 1a**,**b**). We quantified the distribution of the YFP-tagged channels within motor axons of a *Thy1*::*ChR2* mouse by examining cross-sections of the sciatic nerve both parallel and perpendicular to the long axis of the motor axons (**Fig. 1a**,**b**). Nodal and internodal regional anatomy and morphology appeared normal, indicative of a suitable preparation for exploration of optical recruitment (**Fig. 1b**). Using confocal microscopy, we found no correlation between axon size and fluorescent intensity in the transverse sections (**Fig. 1c**, $R^2 = 0.0021$, $P = 0.88$). The observed ChR2-YFP fusion protein abundance was found to systematically

[1]Department of Bioengineering, Stanford University, Stanford, California, USA. [2]Department of Psychiatry and Behavioral Sciences, Stanford University, Stanford, California, USA. [3]Department of Mechanical Engineering, Stanford University, Stanford, California, USA. Correspondence should be addressed to S.L.D. (delp@stanford.edu) or K.D. (deissero@stanford.edu).

Received 11 January; accepted 30 June; published online 26 September 2010; doi:10.1038/nm.2228

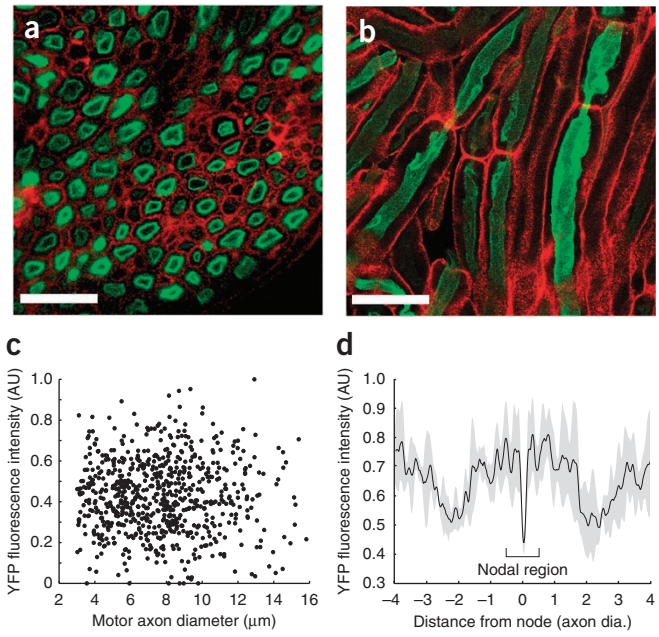


**Figure 1** ChR2 in mouse sciatic nerve. (**a**) Confocal image of sciatic nerve in cross-section. Red, fluorescently labeled laminin of the basal lamina of the peripheral nerve. Green, YFP fluorescence expressed from ChR2-YFP fusion protein expressed under control of the *Thy1* promoter. Scale bar, 50 μm. (**b**) Confocal image of sciatic nerve in longitudinal section; staining as in **a**, illustrating several nodes of Ranvier. Scale bar, 50 μm. (**c**) YFP fluorescence intensity versus motor axon size in cross-section ($n = 4$). (**d**) Average YFP fluorescence intensity parallel to the long axis of sampled axons, where the origin indicates the center of the node of Ranvier ($n = 15$, shaded region represents s.d.).

vary along the axolemma (**Fig. 1d**), with a distribution well suited to the prospect of optical control; the fluorescence intensity at the center of the nodal region represented a minimum along the internodal distance (probably owing to local packing of $Na^+$ channels)[14], whereas the fluorescence intensity in the perinodal region represented a maximum.

### Force and electromyographic response to optical stimulation

We next characterized motor unit recruitment in these mice using optical stimulation by measuring whole-muscle parameters *in vivo*. In large animals such as cats, motor unit recruitment can be characterized by first isolating individual motor units at the ventral root to determine motor unit type by their contractile properties. Once the motor units have been typed, their recruitment order can be determined pairwise by stimulation known to elicit orderly recruitment, such as a homonymous muscle stretch reflex[1,15]. In small animals such as mice, however, this technique is impractical. We therefore used optical or electrical cuffs around the sciatic nerve in *Thy1::ChR2* or control mice (**Fig. 2**). Stimuli provided via the cuffs evoked electrical and contractile responses of the muscle. We measured muscle electrical response (M wave) by fine-wire electromyographic (EMG) electrodes placed in a belly-tendon configuration, whereas we measured contractile force output by a force transducer attached to the Achilles tendon (**Fig. 2a** and **Supplementary Methods**). The medial gastrocnemius, the lateral gastrocnemius and the soleus have free tendons that attach to the distal end of the Achilles tendon. To measure medial gastrocnemius muscle forces (**Figs. 2** and **3**), we detached the free tendons of the other muscles not being measured from the Achilles tendon and manually separated the medial gastrocnemius from the adjacent muscles without interrupting the neurovascular supply to the medial gastrocnemius.

The tetanus response generated by optical stimulation (**Fig. 2a** and **Supplementary Fig. 1**) differs from a typical electrically stimulated tetanus response. The steady-state force value during a tetanus response from optical stimulation approached approximately one-half of its initial peak value (**Fig. 2a**). This characteristic mirrors the peak–steady-state relationship of ChR2 channels expressed in neurons when exposed to light[12] and probably does not affect twitch measurements due to the longer time course of this property. The twitch responses generated by optical stimulation from the medial gastrocnemius (**Fig. 2b**) differ from twitches evoked by electrical stimulation in terms of contraction and relaxation times (**Fig. 3c**,**d**). Optical stimulation produced no stimulation artifact in the EMG response. There was no response to optical stimulation in control mice (**Fig. 2b**), indicating that optical stimulation occurs by photostimulation of the ChR2 channels and not by heat or electrical means.

To compare electrical and optical stimulation across a range of intensities, we calculated the rectified integrated EMG (iEMG) from

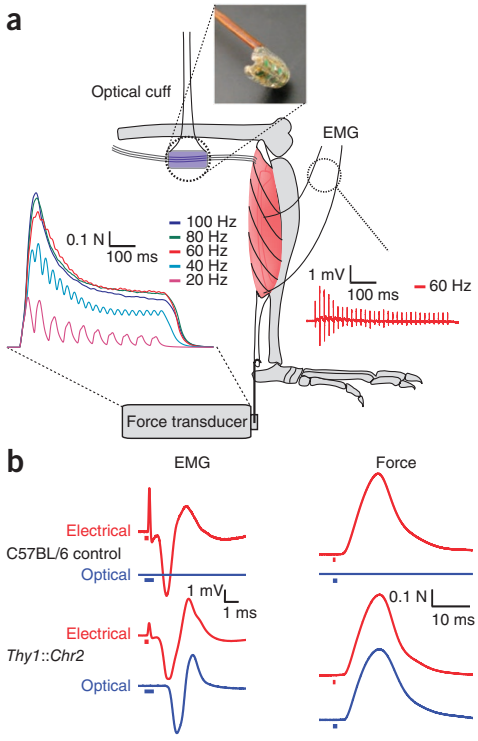


**Figure 2** Optogenetic control of peripheral nerve. (**a**) An optical or electrical cuff is placed around the sciatic nerve of an anesthetized *Thy1::ChR2* mouse. Inset photomicrograph: custom-designed light-emitting diode–based optical cuff. Fine-wire EMG leads are placed in the muscle of interest; EMG plot shows a typical response from optical stimulation. The Achilles tendon is fixed to a force transducer; force traces show typical raw data of contractions at various frequencies of optical stimulation. The sag in force after initial stimulation seen in optical stimulation probably arises from the biophysical properties of the ChR2 channel itself. An example EMG trace is shown for 500 ms at 60 Hz stimulation. (**b**) Typical raw EMG and force traces from twitches elicited by optical and electrical stimulations in *Thy1::ChR2* mice and control C57BL/6 mice. The colored bars near each trace indicate the duration of stimulation.

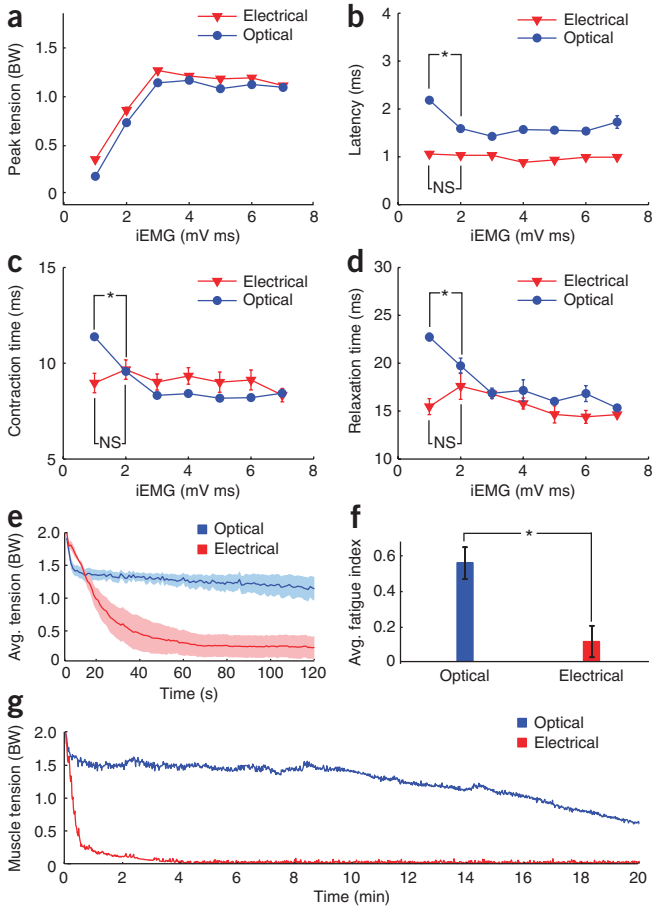


**Figure 3** Orderly recruitment and fatigue resistance with optical stimulation. Each point represents the mean ± s.e.m. (optical, $n = 5$ mice, 625 trials; electrical, $n = 5$ mice, 573 trials; $^*P < 0.01$). Error bars are present at all points and may be smaller than the data-point markers throughout the figure. (**a**) Peak force during a single twitch versus rectified iEMG for both electrical and optical stimulation. (**b**) Average latency measured from initiation of stimuli to detection of EMG. (**c**) Average contraction time measured from 10% of peak force to peak force. (**d**) Average relaxation time measured from peak force to 10% of peak force. (**e**) Average tetanic tension over 2 min in muscle being stimulated with 250-ms trains at 1 Hz using electrical and optical stimulation ($n = 7$, shaded region is s.e.m., average body weight (BW) = 0.258 ± 0.01 N, 2 BW is approximately 20% of maximal isometric tension, **Supplementary Methods**). (**f**) Average fatigue index for electrical and optical stimulation, measured as decline in tetanic tension over 2 min ($n = 7$). (**g**) Exemplar tetanic tension from a single mouse using both optical and electrical stimulation in hindlimbs over 20 min.

raw EMG data over the time interval required for activity to return to within 0.05 mV of zero in each trial and compared average peak force during a twitch to the iEMG response (**Fig. 3a**). The shape of the force relationship under voluntary conditions is thought to be recruitment order dependent[16]; however, we found that overall response characteristics were similar between electrical and optical stimulation. Average peak twitch forces achieved by electrical stimulation were slightly higher than average peak twitch forces with optical stimulation (1.24 ± 0.19 body weights versus 1.12 ± 0.04 body weights; $P < 0.01$; average body weight = 0.258 ± 0.01 N). Twitch forces for both classes of stimulation were also consistent with previous measurements[17,18].

### Measures of orderly recruitment using optical stimulation

Motor axon conduction latency is a widely used measure of motor unit recruitment, given that smaller axons have slower conduction speeds and longer latencies for a given distance[15,19]. Typical measurements of latency record conduction along a nerve only; however, we measured latency (**Fig. 3b**) as the time between the nerve stimulus and the depolarization measured on EMG (M wave), because the physical size of our operative field did not allow us to record from two places along the cut sciatic nerve without introducing error. Latencies measured under optical stimulation for all intensities (ranging from 2.18 ± 0.02 ms to 1.72 ± 0.13 ms) were significantly longer than latencies under electrical stimulation (ranging from 1.15 ± 0.05 ms to 0.99 ± 0.01 ms, $P < 0.01$ in all cases). At the lowest levels of activity (12 mV ms), the latency decreased under optical stimulation ($P < 0.01$) but not under electrical stimulation ($P = 0.11$). This suggested that smaller axons are recruited preferentially at the lowest levels of optical stimulation but not under electrical stimulation. Latency did not decrease with optical stimulation at activities greater than 2 mV ms, presumably because the medial gastrocnemius is innervated by only a small fraction of small motor units[20].

Other measures of motor unit recruitment, the contraction and relaxation times[21,22], also suggested orderly recruitment with optical stimulation. Contraction time (**Fig. 3c**), the time required for twitch tension to increase from 10% of peak force to peak force, was significantly longer using optical stimulation (11.1 ± 0.1 ms) at the lowest levels of muscle activity when compared to electrical stimulation (8.8 ± 0.1 ms, $P < 0.01$). In contrast, at the highest levels of muscle activity, contraction time using optical and electrical stimulation was not significantly different (8.3 ± 0.1 ms, $P = 0.60$) (**Fig. 3c**). Furthermore, relaxation time (time required from twitch tension to fall from peak force to 10% of peak force; **Fig. 3d**) was significantly longer at the lowest level of muscle activity using optical stimulation (21.7 ± 0.4 ms) than electrical stimulation (17.4 ± 0.7 ms, $P < 0.01$), whereas relaxation time at the highest levels of muscle activity were not significantly different between the different types of stimulation (14.5 ± 0.1 ms, $P = 0.10$). The measurements of contraction and relaxation times, which are consistent with other data[17,23], both imply that at the lowest levels of muscle activity optical stimulation preferentially recruits slower motor units.

To test whether optical stimulation of muscle elicits less fatigue than electrical stimulation, we measured tetanic tension generated by the plantarflexor group (lateral gastrocnemius, medial gastrocnemius, soleus and plantaris) of mice using optical and electrical stimulation to activate motor units regardless of their origin in a particular muscle. The fatigability of muscle fibers is affected by multiple factors, including the frequency of stimulation, and is known to be highly plastic under chronic electrical stimulation[24]; however, all parameters were held constant between the electrical and optical stimulation, and we assumed no plastic changes during the short time of our trials. At stimulation intensities in each modality that initially elicited a force of two times the body weight for each unfatigued mouse (**Supplementary Methods**), the force generated by the muscle declined much more rapidly with electrical stimulation than with optical stimulation (**Fig. 3e**). Indeed, the fatigue index, defined as the average tetanic tension of the last train divided by the average tetanic tension in the first train, was strikingly smaller in trials using electrical stimulation (0.11 ± 0.09) than in those using optical stimulation (0.56 ± 0.09, $P < 0.01$; **Fig. 3f**). When we extended the fatigue protocol

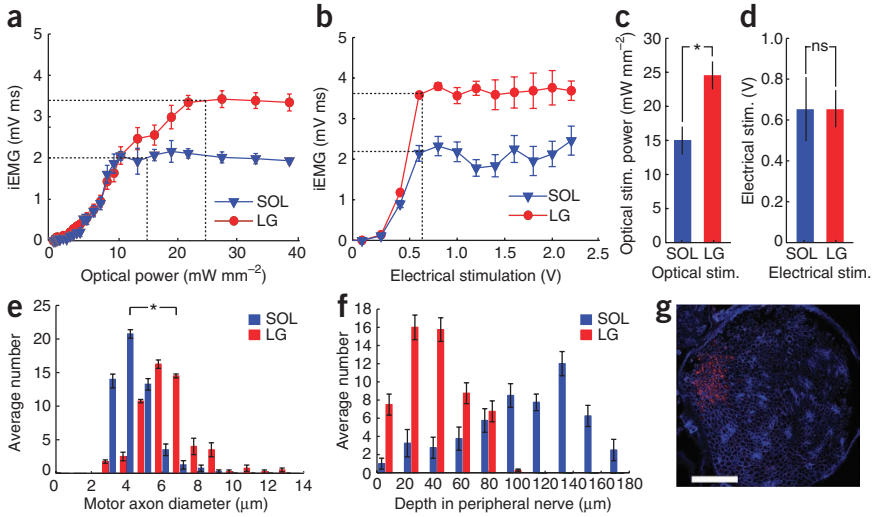


**Figure 4** Differential recruitment of soleus and lateral gastrocnemius with electrical and optical stimulation. Each point represents mean ± s.e.m. (optical, $n = 5$ mice, 1,099 trials; electrical, $n = 5$ mice, 885 trials; $^*P < 0.01$). Error bars are present at all points and may be smaller than the data-point markers throughout the figure. (**a**) Rectified iEMG versus estimated optical intensity at surface of the sciatic nerve for soleus (SOL) and lateral gastrocnemius (LG). (**b**) Rectified iEMG versus electrical stimulation voltage applied to sciatic nerve. (**c**) Optical intensity required to achieve maximum iEMG in soleus and lateral gastrocnemius. (**d**) Electrical stimulation to achieve 95% of maximum iEMG in soleus and lateral gastrocnemius. (**e**) Distribution of motor axon diameters for soleus and lateral gastrocnemius found in cross-section of the sciatic nerve. (**f**) Distribution of soleus and lateral gastrocnemius motor axon depths from the surface of the sciatic nerve. (**g**) Example cross-section of the sciatic nerve where retrograde dye was injected into the lateral gastrocnemius only. Scale bar, 100 μm.

to 20 min in an individual mouse in the contralateral hindlimbs, electrical stimulation diminished tetanic tension completely after 4 min, whereas optical stimulation continued to elicit 32% of the initial tension after the 20-min trial (**Fig. 3g**). These data reveal robustly enhanced performance of the system in the case of optical stimulation, which would be expected from orderly recruitment.

### Recruitment of small motor units with optical stimulation

Differential motor unit recruitment may also enable differential control of distinct muscles that are controlled by the same peripheral nerve. To explore this possibility, we compared the recruitment of two muscles, the soleus and the lateral gastrocnemius (**Fig. 4**). The soleus contains 58 ± 2% slow oxidative fibers and 0% fast glycolytic fibers, whereas the lateral gastrocnemius has 1 ± 3% slow oxidative fibers[20] and 69 ± 13% fast glycolytic fibers. Smaller motor units have smaller axons and tend to have higher compositions of slow oxidative fibers[25], and thus we expected that soleus motor units would be recruited before the faster motor units of the lateral gastrocnemius with larger motor units and larger axons, as reported in other recruitment studies[26]. We found under optical stimulation that soleus (14.9 ± 1.9 mW mm$^{-2}$) reached 95% peak activity at a significantly lower optical intensity than lateral gastrocnemius (**Fig. 4a**,**c**, 24.4 ± 1.9 mW mm$^2$, $P < 0.01$). We also found that the electrical stimulation used to evoke 95% of peak activity in soleus (0.64 ± 0.15 V) and lateral gastrocnemius (0.64 ± 0.09 V) was not significantly different (**Fig. 4b**,**d**, $P = 0.98$). These findings suggest that slower muscle fibers are preferentially recruited by optical stimulation before faster fibers; however, it is impossible to know the order of motor unit recruitment without knowing the size distribution of the motor axons innervating each muscle. Therefore, to analyze axon size distribution and to identify any bias in the location of the axons innervating each muscle within the cross-section of the peripheral nerve, we injected a retrograde dye (Fast Blue) intramuscularly into the muscles of interest to backfill only the axons innervating the muscle in which it was injected[27]. We found in cross-sections of the sciatic nerve (**Fig. 4**) that soleus and lateral gastrocnemius do not contain significantly different numbers of motor axons (**Fig. 4e**, 53.5 ± 4.9 axons for the solueus and 55.0 ± 3.7 axons for the lateral gastrocnemius, $P = 0.71$). However, the average motor axon innervating the lateral gastrocnemius had a significantly larger diameter than those innervating the soleus (6.7 ± 0.16 μm for the solueus and 4.5 ± 0.17 μm for the lateral gastrocnemius, $P < 0.01$). Quantitative histology revealed that soleus axons tended to be at a greater distance from the outer nerve sheath than lateral gastrocnemius axons (**Fig. 4f**), indicating that soleus axons were not exposed to higher intensities of light than lateral gastrocnemius axons (**Supplementary Methods**). These observations support the premise that small motor units are preferentially recruited with optical stimulation and that the observed difference in optical intensity required for peak muscle activity in soleus and lateral gastrocnemius is not influenced by either the number of axons or the position of those axons within the peripheral nerve.

## DISCUSSION

Together, these data demonstrate that optical stimulation achieves the elusive goal of orderly recruitment and can markedly enhance functional performance. The ability to preferentially recruit slower motor units with optical stimulation has potentially enormous functional significance. Functional electrical stimulation systems have been developed to serve as neuroprosthetics for individuals with paralysis but have not been adopted widely in part because of early onset fatigue due to reversed or random motor unit recruitment[7,28]. A number of complex electrical stimulation strategies have been developed that replicate orderly recruitment under controlled circumstances[29,30]. However, optical stimulation of motor neurons is a fundamentally different approach that may solve the motor recruitment problem by stimulating motor units closer to their physiological recruitment pattern without having to suppress large motor units typically required with electrical stimulation. This unique approach is compatible with other forms of optogenetics[31,32], pointing to unprecedented levels of control over motor function. These techniques are currently limited to research in animals; however, recent advances in human gene therapy[33,34] point the way toward eventual clinical applications of this technology. For example, many motor neuron diseases result from overactivity (such as spasticity resulting from cerebral palsy, stroke and traumatic brain injury)[35]; in these cases the light-sensitive $Cl^-$ pump (halorhodopsin) could be employed as an inhibitory gate to control when motor units are activated[36]. Additionally, individual motor units or individual muscles could be essentially 'color-coded' with the devices and principles outlined

here to control individual elements within a muscle volume. This technique opens the door to a vast array of new studies involved in mapping and control of the peripheral nervous system for clinical and bioengineering applications.

## METHODS

Methods and any associated references are available in the online version of the paper at http://www.nature.com/naturemedicine/.

*Note: Supplementary information is available on the Nature Medicine website.*


### ACKNOWLEDGMENTS

We thank R. Barretto and D. Wetmore for technical assistance and K. McGill, Z. Lateva, R. Lieber, D. Lin and F. Zajac for fruitful discussions. This work was supported by a Stanford Bio-X Interdisciplinary Initiatives award (S.L.D. and K.D.), the National Alliance for Research on Schizophrenia and Depression (K.R.T.), and the Stanford–US National Institutes of Health Medical Scientist Training Program (M.E.L.).


### AUTHOR CONTRIBUTIONS

M.E.L. conducted the experiments, performed the analysis and wrote the manuscript. K.R.T. performed the imaging experiments and wrote the manuscript. S.L.D. and K.D. supervised the project and wrote the manuscript.

### COMPETING FINANCIAL INTERESTS

The authors declare no competing financial interests.

Published online at http://www.nature.com/naturemedicine/.
Reprints and permissions information is available online at http://npg.nature.com/reprintsandpermissions/.


1. Burke, R.E., Levine, D.N., Tsairis, P. & Zajac, F.E. III. Physiological types and histochemical profiles in motor units of the cat gastrocnemius. *J. Physiol. (Lond.)* **234**, 723–748 (1973).
2. Henneman, E. Relation between size of neurons and their susceptibility to discharge. *Science* **126**, 1345–1347 (1957).
3. Henneman, E., Somjen, G. & Carpenter, D.O. Functional significance of cell size in spinal motoneurons. *J. Neurophysiol.* **28**, 560–580 (1965).
4. Gordon, T., Thomas, C.K., Munson, J.B. & Stein, R.B. The resilience of the size principle in the organization of motor unit properties in normal and reinnervated adult skeletal muscles. *Can. J. Physiol. Pharmacol.* **82**, 645–661 (2004).
5. Mendell, L.M. The size principle: a rule describing the recruitment of motoneurons. *J. Neurophysiol.* **93**, 3024–3026 (2005).
6. Bakels, R. & Kernell, D. Matching between motoneurone and muscle unit properties in rat medial gastrocnemius. *J. Physiol. (Lond.)* **463**, 307–324 (1993).
7. Singh, K., Richmond, F.J. & Loeb, G.E. Recruitment properties of intramuscular and nerve-trunk stimulating electrodes. *IEEE Trans. Rehabil. Eng.* **8**, 276–285 (2000).
8. Fang, Z.P. & Mortimer, J.T. Selective activation of small motor axons by quasi-trapezoidal current pulses. *IEEE Trans. Biomed. Eng.* **38**, 168–174 (1991).
9. Lertmanorat, Z. & Durand, D.M. Extracellular voltage profile for reversing the recruitment order of peripheral nerve stimulation: a simulation study. *J. Neural Eng.* **1**, 202–211 (2004).
10. Hamada, T., Kimura, T. & Moritani, T. Selective fatigue of fast motor units after electrically elicited muscle contractions. *J. Electromyogr. Kinesiol.* **14**, 531–538 (2004).
11. Zhang, F., Aravanis, A.M., Adamantidis, A., de Lecea, L. & Deisseroth, K. Circuit-breakers: optical technologies for probing neural signals and systems. *Nat. Rev. Neurosci.* **8**, 577–581 (2007).
12. Boyden, E.S., Zhang, F., Bamberg, E., Nagel, G. & Deisseroth, K. Millisecond-timescale, genetically targeted optical control of neural activity. *Nat. Neurosci.* **8**, 1263–1268 (2005).
13. Wang, H. *et al.* High-speed mapping of synaptic connectivity using photostimulation in channelrhodopsin-2 transgenic mice. *Proc. Natl. Acad. Sci. USA* **104**, 8143–8148 (2007).
14. Rasband, M.N. & Trimmer, J.S. Developmental clustering of ion channels at and near the node of Ranvier. *Dev. Biol.* **236**, 5–16 (2001).
15. Zajac, F.E. & Faden, J.S. Relationship among recruitment order, axonal conduction velocity and muscle-unit properties of type-identified motor units in cat plantaris muscle. *J. Neurophysiol.* **53**, 1303–1322 (1985).
16. Fuglevand, A.J., Winter, D.A. & Patla, A.E. Models of recruitment and rate coding organization in motor-unit pools. *J. Neurophysiol.* **70**, 2470–2488 (1993).
17. Kan, H.E. *et al.* Lower force and impaired performance during high-intensity electrical stimulation in skeletal muscle of GAMT-deficient knockout mice. *Am. J. Physiol. Cell Physiol.* **289**, C113–C119 (2005).
18. Zhan, W.Z. *et al.* Effects of genetic selection and voluntary activity on the medial gastrocnemius muscle in house mice. *J. Appl. Physiol.* **87**, 2326–2333 (1999).
19. McPhedran, A.M., Wuerker, R.B. & Henneman, E. Properties of motor units in a heterogeneous pale muscle (m. gastrocnemius) of the cat. *J. Neurophysiol.* **28**, 85–99 (1965).
20. Burkholder, T.J., Fingado, B., Baron, S. & Lieber, R.L. Relationship between muscle fiber types and sizes and muscle architectural properties in the mouse hindlimb. *J. Morphol.* **221**, 177–190 (1994).
21. Cope, T.C. & Clark, B.D. Motor-unit recruitment in the decerebrate cat: several unit properties are equally good predictors of order. *J. Neurophysiol.* **66**, 1127–1138 (1991).
22. Milner-Brown, H.S., Stein, R.B. & Yemm, R. The orderly recruitment of human motor units during voluntary isometric contractions. *J. Physiol. (Lond.)* **230**, 359–370 (1973).
23. Allen, D.G. & Westerblad, H. The effects of caffeine on intracellular calcium, force and the rate of relaxation of mouse skeletal muscle. *J. Physiol. (Lond.)* **487**, 331–342 (1995).
24. al-Amood, W.S., Lewis, D.M. & Schmalbruch, H. Effects of chronic electrical stimulation on contractile properties of long-term denervated rat skeletal muscle. *J. Physiol. (Lond.)* **441**, 243–256 (1991).
25. Burke, R.E., Levine, D.N. & Zajac, F.E. Mammalian motor units: physiological-histochemical correlation in three types in cat gastrocnemius. *Science* **174**, 709–712 (1971).
26. Sokoloff, A.J., Siegel, S.G. & Cope, T.C. Recruitment order among motoneurons from different motor nuclei. *J. Neurophysiol.* **81**, 2485–2492 (1999).
27. Hayashi, A. *et al.* Retrograde labeling in peripheral nerve research: it is not all black and white. *J. Reconstr. Microsurg.* **23**, 381–389 (2007).
28. Thrasher, A., Graham, G.M. & Popovic, M.R. Reducing muscle fatigue due to functional electrical stimulation using random modulation of stimulation parameters. *Artif. Organs* **29**, 453–458 (2005).
29. Fang, Z.P. & Mortimer, J.T. A method to effect physiological recruitment order in electrically activated muscle. *IEEE Trans. Biomed. Eng.* **38**, 175–179 (1991).
30. Zhou, B.H., Baratta, R. & Solomonow, M. Manipulation of muscle force with various firing rate and recruitment control strategies. *IEEE Trans. Biomed. Eng.* **34**, 128–139 (1987).
31. Zhang, F. *et al.* Red-shifted optogenetic excitation: a tool for fast neural control derived from *Volvox carteri*. *Nat. Neurosci.* **11**, 631–633 (2008).
32. Berndt, A., Yizhar, O., Gunaydin, L.A., Hegemann, P. & Deisseroth, K. Bi-stable neural state switches. *Nat. Neurosci.* **12**, 229–234 (2009).
33. Bainbridge, J.W. *et al.* Effect of gene therapy on visual function in Leber's congenital amaurosis. *N. Engl. J. Med.* **358**, 2231–2239 (2008).
34. Maguire, A.M. *et al.* Safety and efficacy of gene transfer for Leber's congenital amaurosis. *N. Engl. J. Med.* **358**, 2240–2248 (2008).
35. McClelland, S., Teng, Q., Benson, L.S. & Boulis, N.M. Motor neuron inhibition–based gene therapy for spasticity. *Am. J. Phys. Med. Rehabil.* **86**, 412–421 (2007).
36. Gradinaru, V. *et al.* Molecular and cellular approaches for diversifying and extending optogenetics. *Cell* **141**, 154–165 (2010).

## ONLINE METHODS

**Nerve microscopy.** Fresh mouse sciatic nerve was fixed in 4% paraformaldehyde for 30 min and washed in PBS. The samples were then embedded in 5% low–melting-point agarose and cut (into 50-μm slices) with a vibratome. The sections were labeled with antibodies to tau (Abcam) and lamin (Dako). The sections were imaged on a confocal microscope (Leica, DM6000). The number, size and fluorescence intensity of the motor axons (≥3 μm and G ratio ≥ 0.5)[37,38] were determined by manual analysis in ImageJ (US National Institutes of Health).

***In vivo* studies.** All studies were approved by Stanford University Institutional Animal Care and Use Committee. Normal-appearing, lab-bred 9-12-week-old *Thy1-ChR2* or C57BL/6 control mice were anesthetized, and the hindlimb was shaved and fixed in a frame. The Achilles tendon was freed by cutting the distal end of the calcaneous to a force transducer (Aurora Scientific, 300C-LR) by thin steel wire. An optical cuff, made of 16 light-emission diodes (Rohm, SMLP12BC7T, 465 nm) arranged in a concentric perimeter facing the peripheral nerve center, or a bipolar hook electrical cuff was inserted around the exposed sciatic nerve that was cut proximal to the site of stimulation (**Supplementary Fig. 1**). In most cases, optical and electrical stimulation were conducted in the same leg at different times. Stainless steel hook electrodes were inserted for differential EMG recordings. EMG recordings were filtered in hardware only (BP 33000 Hz). All force, EMG and stimuli data were sampled at 100 kHz.

All other data analysis was conducted in Matlab. All data reported for the medial gastrocnemius was broken in arbitrarily defined bins on the basis of iEMG value. To determine stimuli needed for 95% maximum iEMG in soleus and lateral gastrocnemius, a Weibull cumulative distribution function was fit to data points. The confidence interval generated by the curve fit was used to define the 99% confidence interval of the required stimuli.

Samples tested for statistically significant differences were first tested for normality with the Lilliefors test ($\alpha = 0.05$) and then tested with the unpaired two-tailed Student's *t* test ($\alpha = 0.05$). All sample groups tested were found to be of normal distribution, except for the axon size data, which was tested with the Mann-Whitney *U* test. All data points listed are mean ± s.e.m. or data ± 99% confidence interval (**Fig. 4c**,**d**).


37. Irintchev, A., Draguhn, A. & Wernig, A. Reinnervation and recovery of mouse soleus muscle after long-term denervation. *Neuroscience* **39**, 231–243 (1990).
38. McHanwell, S. & Biscoe, T.J. The sizes of motoneurons supplying hindlimb muscles in the mouse. *Proc. R. Soc. Lond. B Biol. Sci.* **213**, 201–216 (1981).





doi:10.1038/nm.2228